

Article

An Experimental Study on the Distribution of Grease in Cylindrical Roller Bearings

He Liang ¹, Yan Lu ¹, Wenzhong Wang ^{1,*} , Yi Sun ², Jingjing Zhao ² and Yulong Guo ³

¹ School of Mechanical Engineering, Beijing Institute of Technology, Beijing 100081, China; lianghe@bit.edu.cn (H.L.); luyanbit@163.com (Y.L.)

² Grease Research Institute SINOPEC Co., Ltd., Tianjin 300480, China; syi.lube@sinopec.com (Y.S.); zhaojj.lube@sinopec.com (J.Z.)

³ China Machinery Engineering Corporation, Beijing 100073, China; guoyl@cmecc.com

* Correspondence: wangwzhong@bit.edu.cn

Abstract: The lubrication performance of bearings is greatly influenced by the distribution of the lubricant. In this study, a cylindrical rolling bearing test rig was constructed and presented. The distribution of grease and lubricating oil along the contact region was examined using the laser-induced fluorescence technique, and the thickness of the layer was determined. The lubricating oil and grease layer thickness distribution map was acquired. The effects of supply amount, thickener content, and speed on grease distribution were examined. Mechanisms for replenishing the line contact area were investigated.

Keywords: cylindrical roller bearings; laser-induced fluorescence; grease distribution; layer thickness distribution

1. Introduction

Rolling bearings are key components in mechanical equipment. About 80% of rolling bearings use grease as a lubricant. Traditional research mostly focuses on film formation in the contact area. Wilson [1] thought that the thickness of the grease film can be calculated by using “apparent viscosity”, which was approximately 35% to 50% higher than the viscosity of the corresponding base oil. Astrom et al. [2], under identical conditions, found that the grease film thickness in the contact area was greater than the base oil film thickness. In a ball-on-disc test, the grease’s film thickness is significantly thicker than the base oil’s at very low speeds [3,4]. In bearing experiments, Dong et al. [5] noted the same effect. Cann [6] discovered that increasing speed, viscosity, or base oil viscosity would increase the grease film thickness, while increasing the temperature or working time would decrease it. The aforementioned findings are mostly predicated on an assumption of fully flooded conditions.

Poon [7] found that the film thickness of grease decreased over time. When Coy et al. [8] compared the thrust bearing film thickness measurements with the ball-on-disc test, they found that the major cause of the bearing’s decreasing thickness was an inadequate supply of grease in the contact region. Utilizing the optical method, Chennai M et al. [9] found that the oil film thickness in the contact area of a model bearing is lower than that predicted by the elastohydrodynamic lubrication (EHL) theory due to oil starvation. Gonçalves et al. [10] discovered that as soon as starvation starts, the grease film thickness decreases with increasing speed. Once the supply is limited, the central film thickness in the contact starts to decrease. This indicates that the distribution of the supply layer outside the contact has an impact on the film thickness. Liang et al. [11] found that the geometric structure and wetting performance of the cage directly affect the distribution of lubricating oil in ball bearings. Aamer et al.’s [12] combination of experimental investigation and multiphase CFD model calculations demonstrated the importance of lubricant surface



Citation: Liang, H.; Lu, Y.; Wang, W.; Sun, Y.; Zhao, J.; Guo, Y. An Experimental Study on the Distribution of Grease in Cylindrical Roller Bearings. *Lubricants* **2024**, *12*, 145. <https://doi.org/10.3390/lubricants12050145>

Received: 12 March 2024

Revised: 8 April 2024

Accepted: 20 April 2024

Published: 25 April 2024



Copyright: © 2024 by the authors. Licensee MDPI, Basel, Switzerland. This article is an open access article distributed under the terms and conditions of the Creative Commons Attribution (CC BY) license (<https://creativecommons.org/licenses/by/4.0/>).

tension in the striation patterns across the ball surface. In roller bearings, it can be found that the selection of cage geometry significantly affects lubrication [13]. Sakai et al. [14] found that the type of thickener affects the distribution of the film. The thinner and longer the fibers of the thickener, the easier it is to enter the contact area, thereby increasing the film thickness. Tichy et al. [15] proposed a new model for grease lubrication, which takes into account the fact that grease is a two-component mixture consisting of a thickener and a base oil. Fischer, Jacobs, and colleagues [16] examined how the capillary number (Ca) affected the replenishment and dispersion of oil. Chen et al. [17] developed an air–oil interfacial flow pattern for ball bearings based on Computational Fluid Dynamics (CFD), and found a direct correlation between the capillary number (Ca) and the distribution pattern of lubricating oil around the ball bearing contact region.

By setting a small sapphire window on the rolling track, Pemberton et al. [18] investigated film formation in the contact area between the rollers and the outer ring for cylindrical roller bearings. The experimental results indicated that the oil ribs at the two sides of the contact have little effect on the inlet oil supply. As the rollers orbit in the bearing, they pass the loaded section and the unloaded section. Layers can be generated on the track due to the rollers' passage through the unloaded section and then can replenish the contact directly. As a result, the oil is primarily supplied circumferentially rather than axially from the roller ends. Chen et al. [19] captured images of the distribution of grease near the inlet and found that the degree of oil starvation is related to the distribution of grease fingers on the track. Huang et al.'s ball-on-disc test [20,21] suggested that during rotation, the grease in the outlet may return to the vicinity of the track, resulting in an additional layer of grease and an increase in film thickness. Jiang et al. [22] found that the distribution is an important factor in oil supply at the inlet. Under the oil starvation state, the effect of the capillary force on oil supply in the contact area cannot be ignored. Han et al. [23] found that micro forces such as capillary forces might be a mechanism for oil supply in the contact area under oil starvation.

Academics are still looking for more efficient ways to show the flow and distribution of grease in rolling bearings. The capacitance approach was employed by Cen et al. [24,25] to determine the film thickness of deep groove ball bearings subjected to radial loading. Even though just the average value is available, it is nevertheless able to depict the change in film thickness at high speeds. The thickness of films can also be measured using the ultrasonic approach [26,27]. Li et al.'s [28] results for cylindrical roller bearings showed that the minimum film thickness would grow with increasing speed and decrease with increasing load. Noda et al. [29] observed the interior grease distribution of bearings using the X-ray approach. This method merely observes the stationary situation.

In order to investigate lubrication mechanisms, optical techniques are frequently employed in laboratories because of their great accuracy and spatial resolution. Distribution information may be immediately observed using an optical microscope [30,31]. Under an isoviscous elastic regime, Fowell et al. [32] used the laser-induced fluorescence technique to measure lubricant film thickness in compliant contacts. Franken et al. [33] added different fluorescent dyes to the lubricating medium, and used fluorescence emission spectroscopy to analyze the migration of grease. Our research group has developed a new calibration method for the laser-induced fluorescence technique [34] to improve its precision. The method has successfully been used to detect the distribution characteristics in ball bearings and to obtain the film thickness distribution near the contact and on the free surface [34].

At present, theoretical research can clearly express the relationship between inlet supply conditions and film formation in the contact area. However, for rolling bearings, the distribution and migration of grease cause changes in inlet supply conditions and have an important influence on the bearing lubrication mechanism. This article mainly studies the lubrication distribution of grease in cylindrical roller bearings. Laser-induced fluorescence technology was used to measure the layer thickness, and a high-speed camera was used to directly observe the distribution of grease near the contact area between the roller and the outer ring. The distribution characteristics of lubricating oil and grease were compared,

and the effects of speed, thickener content, and grease filling amount on the distribution of grease were analyzed. The reflow behavior of the line contact area was discovered and verified.

2. Experimental

Figure 1 shows a custom-made rolling bearing test rig. The inner ring was driven by a servo motor and the rotating speed ranged from 10 to 1000 r/min in this study. The test bearing was a cylindrical roller bearing (type: N208; number of rollers: $z = 14$). It has flanges at both ends on the inner ring but no flanges on the outer ring. The outer ring was replaced by a glass flat ring with no grooves for optical observation. The bearing was radially loaded upwards by a stepper motor. The radial load was 380 N and the corresponding maximum Hertzian contact pressure was 169 MPa. The test temperature was 24 ± 1 °C. The experimental conditions are shown in Table 1. PAO8 and lithium grease based on PAO8 were utilized as the lubricating medium. The content of the thickener ranged from 5% to 15%, labeled as Li5%, Li10%, and Li15%. The supply amount of grease was 1 g~3 g, with a volume proportion of 4–13% for grease filling. The grease was supplied to the space between the cage and the inner track, as shown in Figure 1.

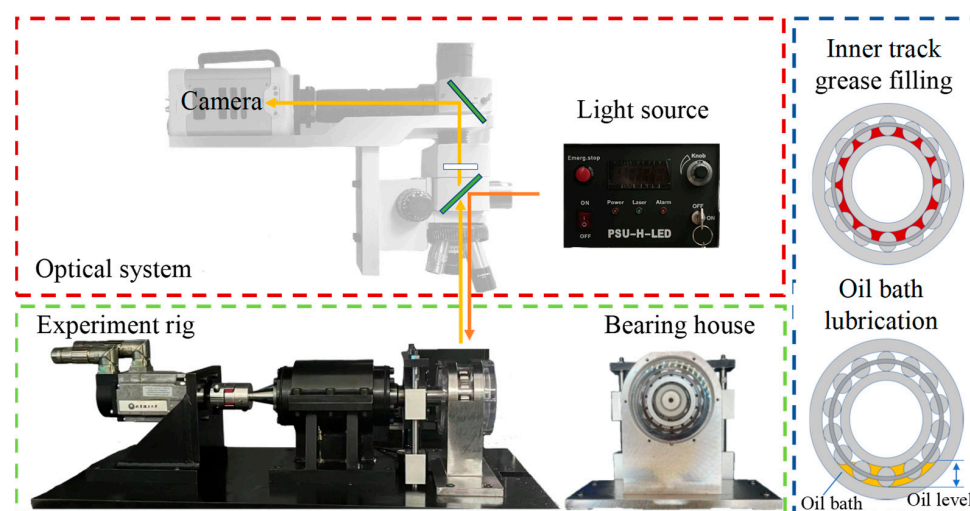


Figure 1. Diagram of the rolling bearing test rig.

Table 1. Experimental conditions and parameters.

	Roller of the Bearing	Glass Ring
Elastic Young's modulus (GPa)	210	75
Poisson ratio	0.293	0.215
Radius (mm)	5.5	35.75
Grease supply (g)		1~3
Temperature t_0 (°C)		24 ± 1

The laser-induced fluorescence technique was applied to observe the distribution of the lubricating medium on cylindrical roller bearings. The optical system is also shown in Figure 1. The fluorescent image of the lubrication medium was excited by a 532 nm laser light source, gathered by a fluorescence microscope, and finally recorded by a high-speed image sensor (CCD).

When fluorescent substances are irradiated by a laser, the electrons surrounding the nucleus absorb energy and transition to an excited state. This excited state is unstable and electrons will return to the ground state, release photons, and generate fluorescence.

There is a corresponding relationship between fluorescence intensity and fluorescence fluid thickness as follows [35]:

$$I_f(h) = kI_0\Phi\{1 - \exp[-\varepsilon(\lambda_{\text{laser}})Ch]\} \quad (1)$$

where I_f is the fluorescence intensity captured by the camera, k is the monitoring efficiency of the camera, I_0 is the intensity of the excitation light at wavelength λ_{laser} , Φ is the dye's quantum efficiency, $\varepsilon(\lambda_{\text{laser}})$ is the molar extinction coefficient of the dye, C is the molar concentration of the dye dissolved in the fluid, and h is the oil layer thickness. According to Equation (1), the layer thickness h at a certain point is exponentially related to the fluorescence intensity received by the camera.

The correlation between the fluorescence intensity and the thickness of the layer may be determined by following these steps: First, the bearing is kept in a fixed position, and then, the grease is injected into the bearing. Once the bearing is subjected to radial load, a line contact area can be established between the roller and the glass ring, and the grease around this contact can create a reservoir. Since the roller is symmetrical, just half of the contact between the roller and the ring is depicted in Figure 2a. A white dashed line delineates the geometry of the reservoir. By defining the center of the roller as the origin, the roller axis as the x -axis, and the radial direction as the y -axis, we can visually represent the gap between the cylindrical roller and the glass ring along the y -axis cross-section in Figure 2b. The layer thickness at a specific location in the reservoir is considered equal to the gap between the roller and the glass ring. The clearance may be determined using the geometric profile and Hertz contact theory, while the fluorescence intensity can be extracted from the pictures recorded by a high-speed camera and analyzed as grayscale values using image processing software.

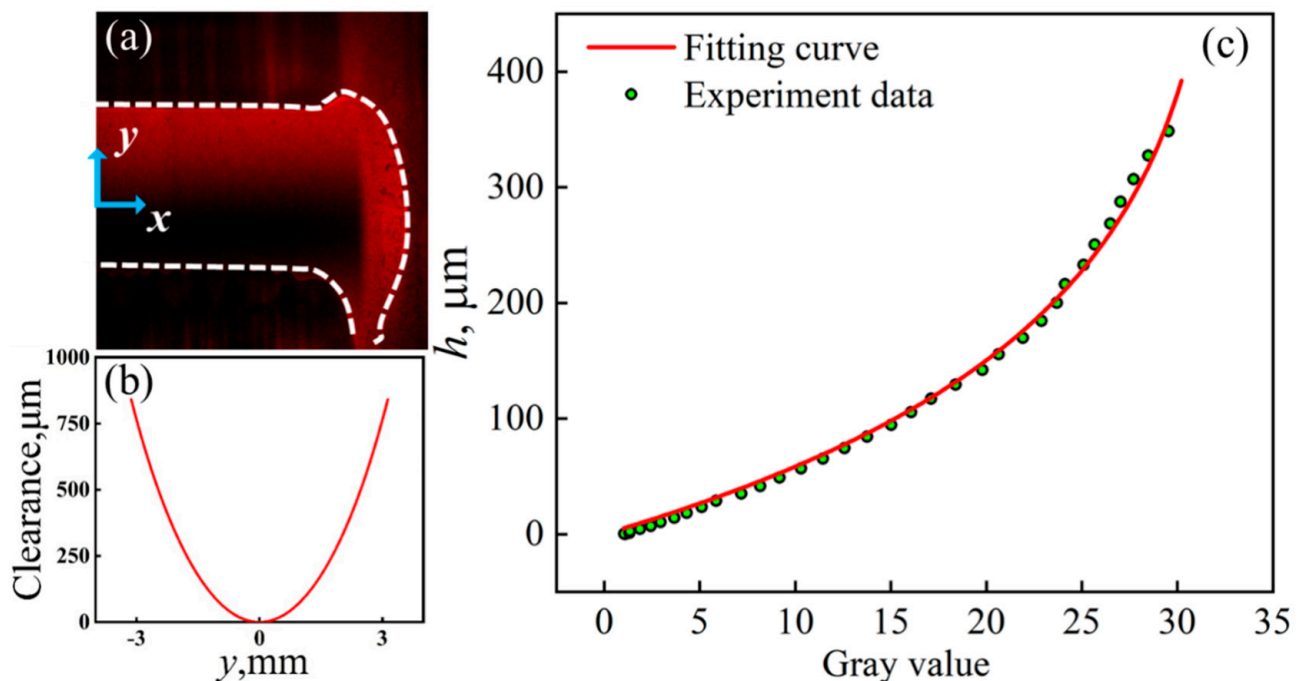


Figure 2. Schematic diagram of fluorescence calibration method and fitting curve of relationship between grayscale values and theoretical clearance: (a) static image of the grease reservoir; (b) calculated clearance between roller and outer ring against y axis; (c) relationship between the layer thickness and the gray value.

The relationship between the grayscale values measured in the experiment and the corresponding layer thickness can be found, and one example is shown in Figure 2c, which is the calibration procedure necessary for the following tests. According to Equation (1),

$kI_0\Phi$ and $\varepsilon(\lambda_{\text{laser}})C$ are considered constant, and the fitting result can be given by the following expression:

$$h = -0.16338 * \ln(1 - 0.03009 * I_f(h)) \quad (2)$$

The fitting degree $R^2 = 0.99601$. Equation (2) has a good fit with the experimental data. Recalibration is performed for each experiment to avoid the influence of external environmental changes on the fitting parameters.

3. Experimental Results

3.1. The Preparation of the Lubricating Medium

To increase the fluorescence intensity, a fluorescent dye was dissolved in the lubricant. For the lubricating oil, the powder of the fluorescent dye was added into the oil directly, and then, they were sonicated at 60 °C for 30 min or longer so that the dye was dissolved evenly.

Fluorescent dye cannot be directly dissolved in grease. The mechanical rolling method was used among the various tried methods: a certain amount of fluorescent dye was mixed and stirred with grease first, and then, the mixture was grounded on a three-roll grinder until it became uniform. Figure 3 shows the images of the oil and grease tagged with fluorescent dyes; the color has changed from colorless or white to dark red. The lubricating oil/grease with fluorescent dyes are represented as PAO8-F, Li5%-F, Li10%-F, and Li15%-F. The emission spectra of the lubricating medium tagged with dyes were measured using a spectrometer (Ocean Optics, USB2000+, Orlando, FL, USA) and are shown in Figure 3. Under the irradiation of a 532 nm laser light source, the lubricating medium tagged with dyes can generate fluorescence signals with a wavelength of approximately 650 nm. Figure 4 compares the changes in rheological properties of PAO8 and Li10% as examples. An Anton Paar 301 rheometer was used, with a testing temperature of 24 °C and a shear rate ranging from 0 to 8000·s⁻¹. It can be observed that the overall rheological properties of PAO8 and Li10% show a similar trend after the addition of fluorescent dyes, and their viscosity slightly decreases. The viscosity of the grease is much higher than its base oil viscosity. The yield stresses of Li5%-F, Li10%-F, and Li15%-F are 128 Pa, 1017 Pa, and 1770 Pa, respectively. The higher the thickener content, the greater the yield stress.

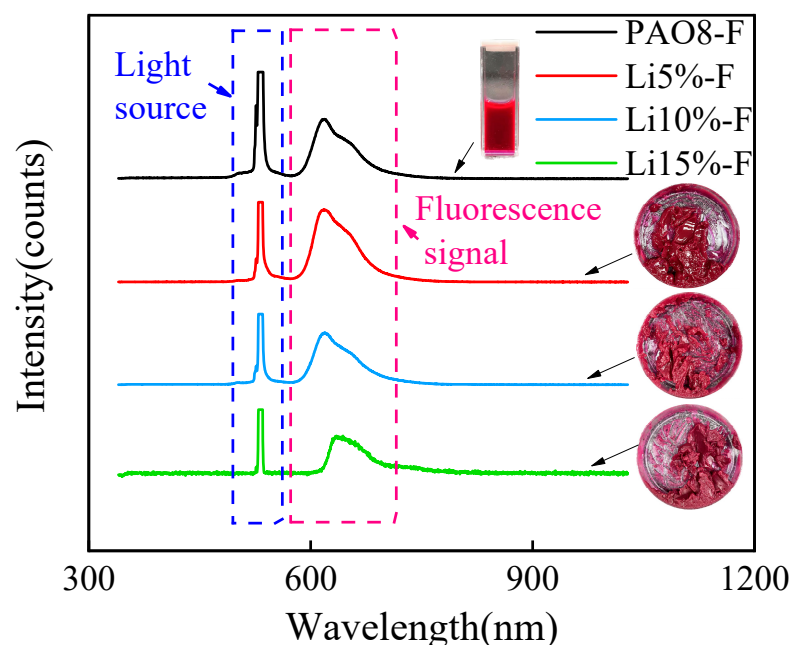


Figure 3. Emission spectrum of the lubricating medium tagged with fluorescent dyes.

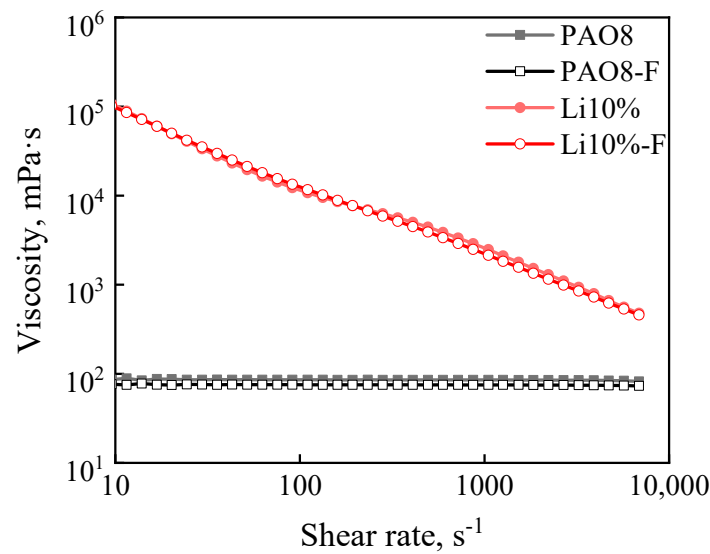


Figure 4. Changes in rheological properties of lubricating oil and grease before and after adding fluorescent dyes.

3.2. The Distribution of the Lubricating Oil

In this section, PAO8 was used as the test lubricating medium, and the area near the contact which was formed by the most loaded roller and the outer ring in the cylindrical roller bearings was mainly focused on. Figure 5 shows the fluorescent image near the contact. The line contact zone is shown by the dashed line. The width of the contact area is approximately 75 μm . Assuming that the distribution of the oil reservoirs along the x -axis can be approximated as a symmetrical distribution, only half of the contact area and the oil reservoir distribution are shown here. According to Equation (1), the fluorescence intensity is positively correlated with the layer thickness. The fluorescence intensity near the contact area is low, indicating that the oil layer is thin. The fluorescence intensity away from the contact area increases gradually, indicating that the oil layer thickness increases gradually.

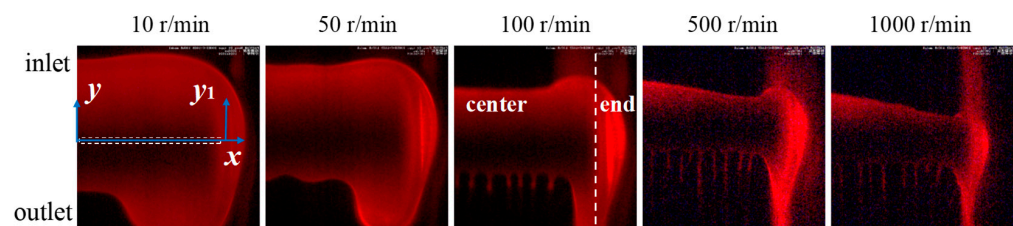


Figure 5. Fluorescent images near the contact area formed by the roller and outer ring at the maximum radial loading point of cylindrical roller bearings: PAO8, 1 g.

The oil reservoir near the contact area can be divided into two parts: the center part and the end part. When the rotating speed is 10 r/min, the center part of the oil reservoir is distributed as a rectangular shape. As the rotating speed increases, the inlet area gradually protrudes, while the outlet area shows fingers. The higher the rotating speed, the thinner the fingers. The end part of the oil reservoir is relatively brighter. As the rotating speed increases, the width of the end part of the oil reservoir gradually decreases, and the length also gradually elongates until it connects to the next oil reservoir and forms an oil belt.

Figure 6 shows the distribution of layer thickness corresponding to the fluorescent images in Figure 5. Due to the obvious variation in layer thickness with rotating speed, two color bars with different thickness ranges were selected. It can be seen that the farther away from the contact area the oil is, the thicker the oil layer. Along the x -axis, the layer thickness distribution is relatively uniform, which conforms to the characteristics of the line contact area. The thickness near the end part is relatively large. When the rotating

speed increases to 500 r/min, the layer thickness near the end part is much greater than the layer thickness in the central part. This indicates that a large amount of lubricating oil is concentrated at the end of the roller.

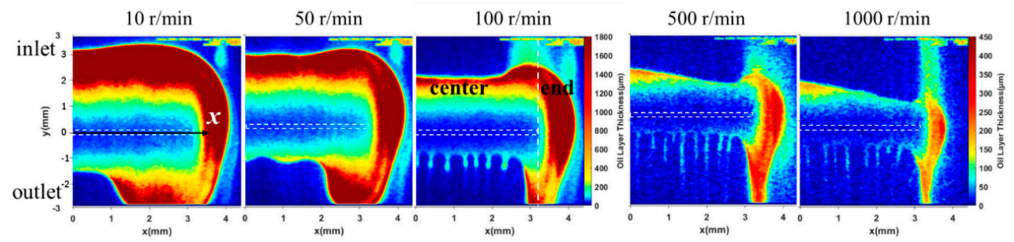


Figure 6. Distribution of layer thickness near contact area: PAO8-F, 1 g.

Figure 7 shows the cross-profile of oil layer thickness along the y -axis. The origin of the coordinates is the center of the contact area. The layer thickness in the inlet area gradually increases and remains consistent with the clearance between the roller and the outer ring. The oil film drops sharply after it reaches the maximum thickness, and the layer thickness on the free surface is only a few micrometers. This indicates that the lubricating oil at the center of the track is mainly concentrated in the oil reservoir and is very thin on free surfaces. The thickest oil film in the central section along the y -axis can be defined as the inlet layer thickness h_{inlet} . The variation in the inlet layer thickness with velocity is shown in Figure 7. The change in the inlet layer thickness is basically consistent with the clearance between the roller and the outer ring. At a speed of 100 r/min, the inlet layer thickness reaches up to 500 μm and fully ensures the oil supply of the contact area. However, as the speed increases, the inlet layer thickness rapidly decreases.

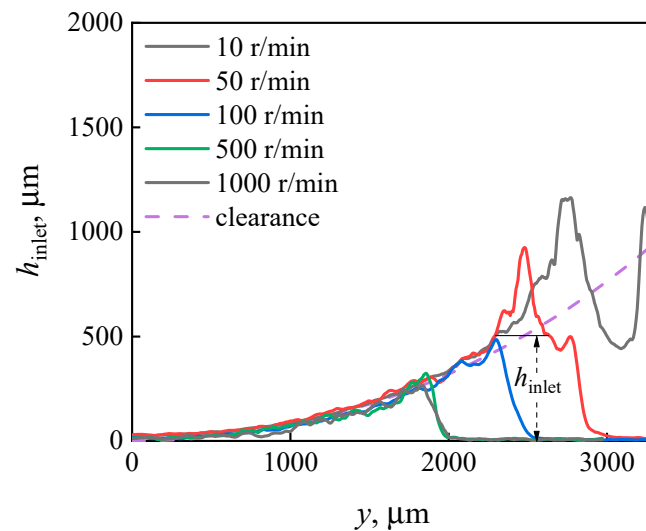


Figure 7. Cross-profile of layer thickness along y -axis.

3.3. The Distribution of the Grease

In this section, lithium grease was used as the test lubricating medium. Figure 8 shows the fluorescent images of grease near the contact area. The grease reservoir can also be divided into a center part and an end part. The grease reservoir in the center part is generally distributed in a rectangular shape. It is similar to the lubricating oil reservoir, but the layer is much thinner. Differently, a large number of grease fingers occur in the outlet area. The grease fingers on the side of the outlet area are thicker and longer than those in the center. The grease fingers become thinner and longer with higher rotating speeds. When the rotating speed exceeds 500 r/min, the layer thickness becomes a few micrometers, and the fluorescent signal is quite weak to distinguish. The grease distribution at the end

part is different from that of oil lubrication, as a grease belt can be formed with a layer thickness up to 200 μm . As the rotating speed increases, both the width of the grease belt and the layer thickness gradually decrease.

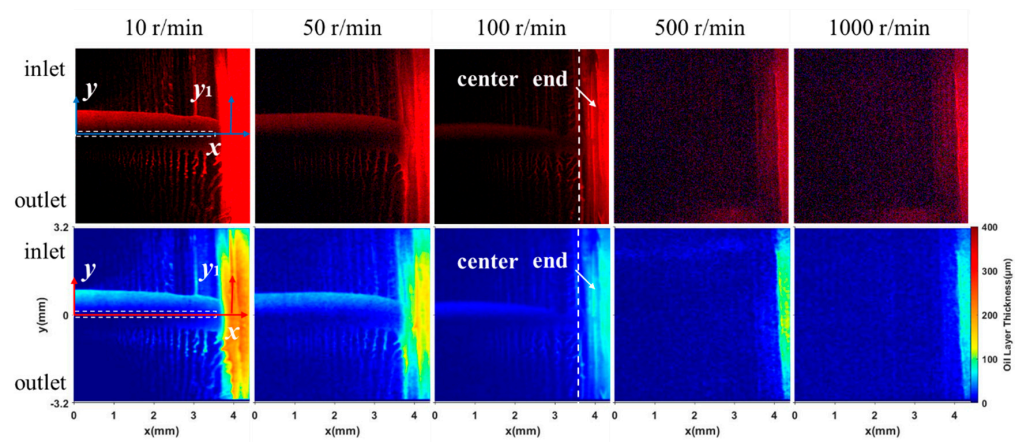


Figure 8. Fluorescent images and the corresponding distribution of layer thickness near the contact area lubricated by the grease. Li10%-F, 1 g.

Figure 9 shows the distribution of the grease layer affected by different thickener contents. The content of the thickener ranges from 5% to 15%. When the thickener content is 5%, the shape of the grease reservoir is similar to that of its base oil, which is rectangular. Short grease fingers can be seen in the outlet area. Most of the grease at the end area concentrates near the contact area to form the grease reservoir. A grease belt is formed at higher rotating speeds when the tail flow of the grease reservoir is elongated. For the thickener content of 10%, the fluidity of the grease deteriorates, and the grease reservoir becomes obviously smaller than that of 5%. The grease fingers in the outlet area have a denser and thinner distribution, and a grease belt is formed in the end area. The fluidity of the grease further deteriorates by increasing the content of the thickener to 15%, and the grease reservoir is almost invisible. Most of the grease is squeezed to the sides of the end and forms a thick grease ridge.

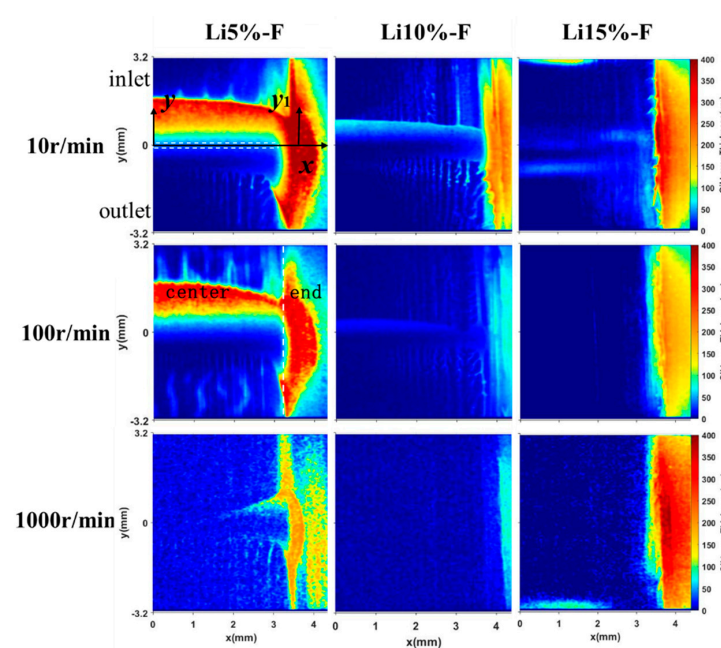


Figure 9. Distribution of layer thickness for grease, with thickener content of 5%, 10%, and 15% at 1 g.

Figure 10a shows the variation in the inlet layer thickness h_{inlet} with different rotating speeds when using grease with different thickener contents. Basically, the thickness of the inlet film gradually decreases with increasing speed except for that of Li15%-F, which slightly increases at low rotating speeds and then rapidly decreases. The inlet layer thickness of PAO8 base oil is the largest, and the higher the content of thickener, the smaller the inlet layer thickness. The $y1$ axis is defined at the center of the grease belt, as shown in Figure 9, and the maximum oil layer along the center section of the $y1$ axis is defined as h_{end} . Figure 10b compares the effect of thickener content on the thickness h_{end} . h_{end} of Li5%-F and Li10%-F shows an overall decreasing trend with increasing speed, while h_{end} of Li15%-F decreases at low speeds and gradually increases thereafter. h_{end} of Li10%-F is the smallest in all situations.

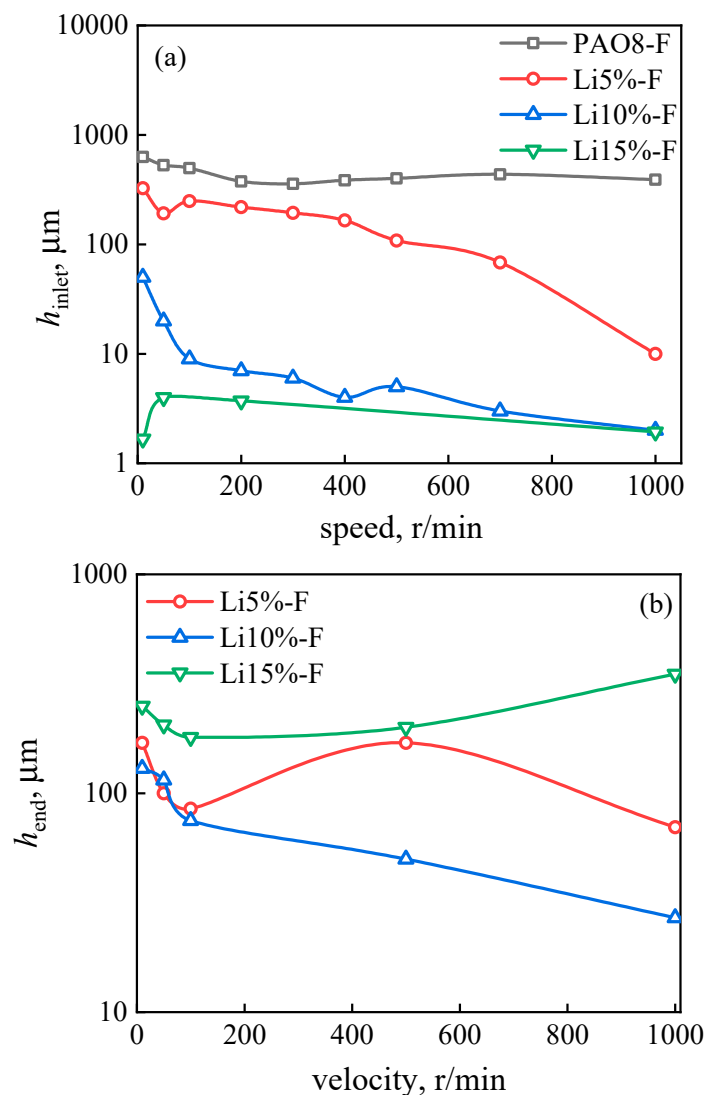


Figure 10. The change in h_{inlet} and h_{end} for PAO8 and grease with different thickener contents against rotational speed. (a) the change of h_{inlet} . (b) the change of h_{end} .

Figure 11 shows the distribution of the grease film affected by the grease filling amount. The observation window was moved 1 mm to the right to observe the full view of the grease belt at the end. The x -axis coordinate range changes to 1~5 mm. At 50 r/min, the increase in grease infillings greatly affects the distribution of the grease layer. The greater the grease infillings, the larger the grease reservoir, the thicker the grease fingers, and the wider the grease belt at the end. At 500 r/min, different grease filling amounts may not cause significant changes in the size of the grease reservoir; the grease layer on the track,

however, gradually thickens with greater grease infillings. The thickness of the grease belt at the end changes imperceptibly, while the width gradually increases.

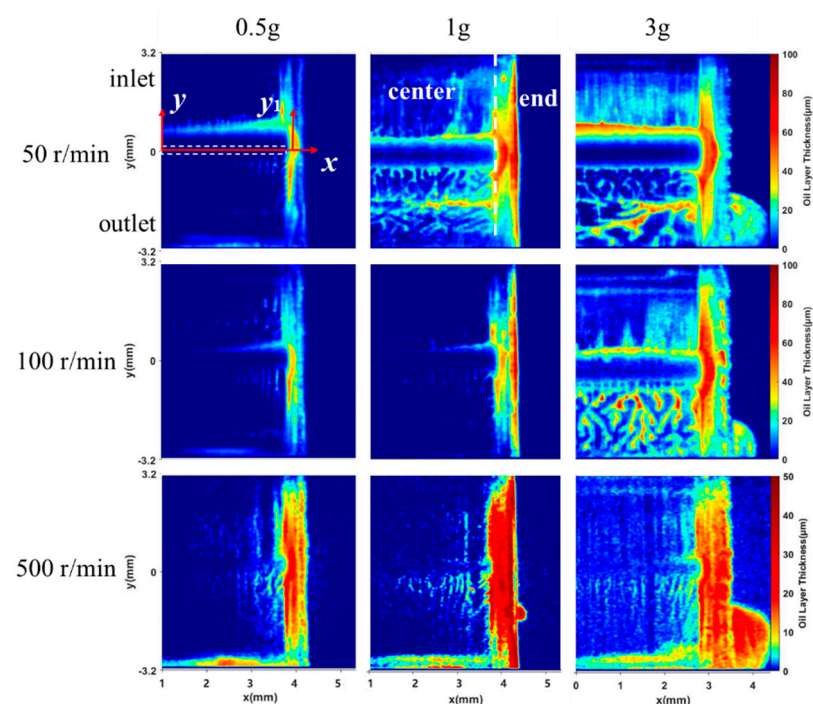


Figure 11. The effect of the grease filling amount on the distribution of oil layer thickness: Li10%-F.

4. Discussion

There are two forms to supply the line contact area: one is the circumferential supply (along the y axis), which means that the grease dispersed on the track can directly supply the line contact area; another form is axial supply (along the x axis), which means that the grease at the end gradually migrates to the reservoir, thereby supplementing the contact area. From the experimental results, the grease reservoir for the line contact area has a rectangular shape for most of the time. It is more like a grease reservoir formed based on circumferential supply, as the grease on the track can be evenly squeezed during axial loading. This result is consistent with the experimental results in reference [18]. Figures 6–10 illustrate that rotating speed is the most important factor in determining the layer thickness of the grease reservoir. The higher the rotating speed, the smaller the h_{inlet} . Figure 11 shows that the grease filling amount has a positive effect on the layer thickness. More grease added to the bearing results in a thicker oil layer on the track.

The experimental results also show that the axial supply for the line contact area cannot be ignored when the grease filling amount is small. As shown in Figure 9, Li5%-F shows a significant decrease in the inlet oil film from the end to the center at 1000 r/min. In Figure 11, a similar situation exists for Li10%-F at a supply of 0.5 g. Taking Li10%-F at supply of 0.5 g in Figure 11 as an example, a small grease reservoir is formed at the end area, and grease fingers are formed in the outlet area developing inward, which may continuously transport grease to the central area. In addition, the position of the tail flow is closer to the center compared to the end of the grease reservoir, which also helps to migrate the grease from the end to the central area during the rolling processes. During the movement of the contact area, the grease reservoir can be replenished by the tail flow left by the previous contact area while leaving a new tail flow. During this process, the lubricating media in different contact areas are replenished and balanced with each other. However, Li15%-F has poor fluidity and lacks such flow and replenishment. It can be seen that the position of the grease belt at the end is basically unchanged, making it difficult to replenish the contact area.

The clearance of the roller end has an adsorption effect on the lubricating medium. According to the analysis in reference [17], it is mainly the effect of capillary force. However, the viscous force prevents the lubricating medium from migrating. For the lubricating oil, PAO8 can quickly converge to the end and forms an oil reservoir. For lithium-based grease, Figure 11 shows that the grease reservoir can be formed at the end at different speeds and with different filling amounts. The layer thickness at the end is thicker than that in the central area. The lower the content of the thickener, the less viscous the lubricating medium is, and the easier it is to converge to the roller end and form a grease reservoir. Figure 9 shows that the shape of the Li5%-F oil reservoir is closer to that of the lubricating oil. On the contrary, the higher the content of the thickener, the greater the viscosity of the lubricating medium. For Li15%-F, there is a thick oil belt near the end, but it is difficult to converge to the roller end for replenishment.

5. Conclusions

By comparing the grease and oil, this work experimentally studied the distribution of supply layers for the line contact area in a cylindrical roller bearing. The laser-induced fluorescence technique was used to measure the layer thickness. The effects of speed, thickener content, and filling amount were studied.

1. The reservoir around the line contact area in a cylindrical roller bearing mainly has a rectangular shape. Rotating speed is the most important factor influencing the layer thickness of the reservoir. Higher speeds lead to smaller reservoirs.
2. There are two lubricant supply modes for the line contact area in a cylindrical roller bearing: circumferential and axial. In general, circumferential supply is the main form; when the supply is very small or when there are higher speeds, it can be observed that the axial supply cannot be ignored.
3. For axial supply, a small grease reservoir can be formed at the end area, and grease fingers are formed in the outlet area developing inward. In addition, different contact areas can be supplemented by the tail flow exchange while migrating to the center.

Author Contributions: Conceptualization, W.W.; Methodology, H.L.; Validation, Y.G.; Investigation, Y.L.; Resources, Y.S. and J.Z. All authors have read and agreed to the published version of the manuscript.

Funding: This work was financially supported by the National Key R&D Program of China (No. 2021YFB2011000) and the National Natural Science Foundation of China (52175158, U2141243, 52305179).

Data Availability Statement: The original contributions presented in the study are included in the article, further inquiries can be directed to the corresponding author.

Acknowledgments: We are grateful to SINOPEC for providing all grease samples for this study.

Conflicts of Interest: Authors Yi Sun and Jingjing Zhao are employed by the company Grease research Institute SINOPEC. Author Yulong Guo is employed by China Machinery Engineering Corporation. The remaining authors declare that the research was conducted in the absence of any commercial or financial relationships that could be construed as a potential conflict of interest.

References

1. Wilson, R.A. The relative thickness of grease and oil films in rolling bearings. *Proc. Inst. Mech. Eng.* **1979**, *193*, 185–192. [[CrossRef](#)]
2. Åström, H.; Isaksson, O.; Höglund, E. Video recordings of an EHD point contact lubricated with grease. *Tribol. Int.* **1991**, *24*, 179–184. [[CrossRef](#)]
3. Morales-Espejel, G.E.; Lugt, P.M.; Pasaribu, H.; Cen, H. Film thickness in grease lubricated slow rotating rolling bearings. *Tribol. Int.* **2014**, *74*, 7–19. [[CrossRef](#)]
4. Kimura, Y.; Endo, T.; Dong, D. EHL with grease at low speeds. In *Advanced Tribology: Proceedings of CIST2008 & ITS-IFTtoMM2008*; Springer: Berlin/Heidelberg, Germany, 2010; pp. 15–19.
5. Dong, D.; Komoriya, T.; Endo, T.; Kimura, Y. Formation of EHL film with grease in ball bearings at low speeds. *J. Jpn. Soc. Tribol.* **2012**, *57*, 568–574.

6. Cann, P. Starved grease lubrication of rolling contacts. *Tribol. Trans.* **1999**, *42*, 867–873. [[CrossRef](#)]
7. Poon, S.-Y. An experimental study of grease in elastohydrodynamic lubrication. *J. Tribol.* **1972**, *94*, 27–34. [[CrossRef](#)]
8. Coy, J.J.; Zaretsky, E.V. Some limitations in applying classical EHD film thickness formulas to a high-speed bearing. *J. Tribol.* **1981**, *103*, 295–301. [[CrossRef](#)]
9. Chennaoui, M.; Fowell, M.; Liang, H.; Kadiric, A. A Novel Set-up for In-situ Measurement and Mapping of Lubricant Film Thickness in a Model Rolling Bearing Using Interferometry and Ratiometric Fluorescence Imaging. *Tribol. Lett.* **2022**, *70*, 85. [[CrossRef](#)]
10. Gonçalves, D.E.; Campos, A.V.; Seabra, J.H. An experimental study on starved grease lubricated contacts. *Lubricants* **2018**, *6*, 82. [[CrossRef](#)]
11. Liang, H.; Zhang, Y.; Wang, W. Influence of the cage on the migration and distribution of lubricating oil inside a ball bearing. *Friction* **2022**, *10*, 1035–1045. [[CrossRef](#)]
12. Aamer, S.; Sadeghi, F.; Russell, T.; Peterson, W.; Meinel, A.; Grillenberger, H. Lubrication, flow visualization, and multiphase CFD modeling of ball bearing cage. *Tribol. Trans.* **2022**, *65*, 1088–1098. [[CrossRef](#)]
13. Aamer, S.; Sadeghi, F.; Meinel, A. Cylindrical roller bearing cage pocket lubrication. *Tribol. Int.* **2023**, *188*, 108851. [[CrossRef](#)]
14. Sakai, K.; Tokumo, Y.; Ayame, Y.; Shitara, Y.; Tanaka, H.; Sugimura, J. Effect of Formulation of Li Greases on Their Flow and Ball Bearing Torque. *Tribol. Online* **2016**, *11*, 168–173. [[CrossRef](#)]
15. Tichy, J.; Menut, M.; Oumahi, C.; Muller, S.; Bou-Saïd, B. Grease flow based on a two-component mixture model. *Tribol. Int.* **2021**, *153*, 106638. [[CrossRef](#)]
16. Fischer, D.; von Goedel, S.; Jacobs, G.; Stratmann, A. Numerical investigation of effects on replenishment in rolling point contacts using CFD simulations. *Tribol. Int.* **2021**, *157*, 106858. [[CrossRef](#)]
17. Chen, H.; Liang, H.; Wang, W.; Zhang, S. Investigation on the oil transfer behaviors and the air-oil interfacial flow patterns in a ball bearing under different capillary conditions. *Friction* **2023**, *11*, 228–245. [[CrossRef](#)]
18. Pemberton, J.; Cameron, A. An Optical Study of the Lubrication of a 65 mm Cylindrical Roller Bearing. *Ind. Lubr. Tribol.* **1979**, *33*, 84–94. [[CrossRef](#)]
19. Chen, J.; Tanaka, H.; Sugimura, J. Experimental Study of Starvation and Flow Behavior in Grease-Lubricated EHD Contact. *Tribol. Online* **2015**, *10*, 48–55. [[CrossRef](#)]
20. Huang, L.; Guo, D.; Wen, S. Film thickness decay and replenishment in point contact lubricated with different greases: A study into oil bleeding and the evolution of lubricant reservoir. *Tribol. Int.* **2016**, *93*, 620–627. [[CrossRef](#)]
21. Huang, L.; Guo, D.; Wen, S.; Wan, G.T.Y. Effects of Slide/Roll Ratio on the Behaviours of Grease Reservoir and Film Thickness of Point Contact. *Tribol. Lett.* **2014**, *54*, 263–271. [[CrossRef](#)]
22. Jian, N.; Li, X.; Yang, P.; Guo, F. Observation of lubrication state and lubricant replenishment under sliding-rolling motions with single-charging amount. *Tribology* **2021**, *41*, 9–16.
23. Han, B.; Wang, W.; Zhao, Z. Oil Replenishment Mechanism of Lubricated Contact at Low Speed. *Tribology* **2016**, *36*, 341–347.
24. Cen, H.; Lugt, M.P. Film thickness in a grease lubricated ball bearing. *Tribol. Int.* **2019**, *134*, 26–35. [[CrossRef](#)]
25. Cen, H.; Lugt, P.M. Replenishment of the EHL contacts in a grease lubricated ball bearing. *Tribol. Int.* **2020**, *146*, 106064. [[CrossRef](#)]
26. Dwyer-Joyce, R.; Reddyhoff, T.; Drinkwater, B. Operating limits for acoustic measurement of rolling bearing oil film thickness. *Tribol. Trans.* **2004**, *47*, 366–375. [[CrossRef](#)]
27. Dou, P.; Jia, Y.; Wu, T.; Peng, Z.; Yu, M.; Reddyhoff, T. High-accuracy incident signal reconstruction for in-situ ultrasonic measurement of oil film thickness. *Mech. Syst. Signal Process.* **2021**, *156*, 107669. [[CrossRef](#)]
28. Li, M.; Liu, H.; Xu, C.; Jing, M.; Dong, G. Ultrasonic measurement of cylindrical roller-bearing lubricant film distribution with two juxtaposed transducers. *Tribol. Trans.* **2017**, *60*, 79–86. [[CrossRef](#)]
29. Noda, T.; Shibasaki, K.; Miyata, S.; Taniguchi, M. X-ray CT imaging of grease behavior in ball bearing and numerical validation of multi-phase flows simulation. *Tribol. Online* **2020**, *15*, 36–44. [[CrossRef](#)]
30. Lugt, P.M.; Velickov, S.; Tripp, J.H. On the chaotic behavior of grease lubrication in rolling bearings. *Tribol. Trans.* **2009**, *52*, 581–590. [[CrossRef](#)]
31. Sato, N.; Sakaguchi, T. Improvement of grease leakage prevention for ball bearings due to geometrical change of ribbon cages. *Tech. Rev.* **2010**, *78*, 91–97.
32. Fowell, M.; Myant, C.; Spikes, H.; Kadiric, A. A study of lubricant film thickness in compliant contacts of elastomeric seal materials using a laser induced fluorescence technique. *Tribol. Int.* **2014**, *80*, 76–89. [[CrossRef](#)]
33. Franken, M.; Chennaoui, M.; Wang, J. Mapping of grease migration in high-speed bearings using a technique based on fluorescence spectroscopy. *Tribol. Trans.* **2017**, *60*, 789–793. [[CrossRef](#)]
34. Chen, H.; Wang, W.; Ge, X.; Liang, H. Pixel-dependent laser-induced fluorescence method for determining thin liquid film thickness distribution. *Phys. Fluids* **2024**, *36*, 012111. [[CrossRef](#)]
35. Hidrovo, C.H.; Hart, D.P. Emission reabsorption laser induced fluorescence (ERLIF) film thickness measurement. *Meas. Sci. Technol.* **2001**, *12*, 467. [[CrossRef](#)]

Disclaimer/Publisher’s Note: The statements, opinions and data contained in all publications are solely those of the individual author(s) and contributor(s) and not of MDPI and/or the editor(s). MDPI and/or the editor(s) disclaim responsibility for any injury to people or property resulting from any ideas, methods, instructions or products referred to in the content.